Research Article | Vol. 29, No. 20 / 27 Sep 2021 / Optics Express 31706
Optics EXPRESS

Electro-optically Q-switched operation of a high-peak-power $Tb:LiYF_4$ green laser

H. YANG,[1] H. CHEN,[2,3] E. LI,[1] H. UEHARA,[1,4] AND R. YASUHARA[1,4,*]

[1] The Graduate University for Advanced Studies, SOKENDAI, 322-6 Oroshi-cho, Toki, Gifu, Japan
[2] School of Mechanical Engineering, University of South China, Hengyang 421001, China
[3] Hunan Province Key Laboratory for Ultra-Fast Micro/Nano Technology and Advanced Laser Manufacture, School of Electrical Engineering, University of South China, Hengyang 421001, China
[4] National Institute for Fusion Science, 322-6 Oroshi-cho, Toki, Gifu, Japan
[*] yasuhara.ryo@nifs.ac.jp

Abstract: We report on an electro-optically Q-switched $Tb:LiYF_4$ green laser pumped by a frequency-doubled optically pumped semiconductor blue laser. The electro-optically Q-switched characteristics were studied under a wide range of repetition rates from 200 Hz to 50 kHz using a KD_2PO_4 Q-switch. Up to 198 μJ of pulse energy was obtained with a pulse width of 248 ns at a repetition rate of 200 Hz, corresponding to a peak power of 797 W at 544 nm.

1. Introduction

Recently, visible green lasers have been attracting significant attention worldwide owing to their potential use not only in our daily life applications (e.g., micro-projectors and laser headlights [1–3]) but also various other fields (e.g., medicine [4,5], display technology [6,7], molecular imaging [8], and laser processing [9,10]). Several rare-earth ions (such as Nd^{3+}, Dy^{3+}, Sm^{3+}, Pr^{3+}, and Tb^{3+}) are used to generate visible lasers either directly or indirectly [3,11–16]. Solid-state Nd^{3+} visible lasers are the most widely used and are produced through nonlinear frequency conversion. For example, an intracavity frequency-doubling electro-optically Q-switched Nd: $LiYF_4$ green laser with a pulse energy of 16.8 mJ and a pulse width of less than 8 ns has been reported [15]. Further, pulse energy up to 9.7 mJ at a repetition rate of 1 kHz was realized using a frequency-doubling electro-optically Q-switched Nd: YAG laser [16]. These operations are known to require a second harmonic generation process to obtain visible lasers, which exhibit relatively low efficiencies. In contrast, Dy^{3+}, Sm^{3+}, Pr^{3+}, and Tb^{3+} have the intrinsic advantage of generating visible lasers directly without nonlinear processes. They can be optically pumped using semiconductor-based blue laser sources. Among them, Pr^{3+} and Tb^{3+} ion-doped lasers have become interesting research topics, owing to their potential use in these applications because their respective energy transitions (i.e., Tb^{3+}: $^5D_4 \rightarrow {}^7F_5$, Pr^{3+}: $^3P_{2,1,0}$, $^1I_6 \rightarrow {}^3H_{6,5}$) can directly produce laser radiation in the green waveband. In addition, note that the upper level of Tb^{3+} ion has a relatively longer lifetime than that of Pr^{3+} ion (typically ~5 ms for Tb^{3+} ions and ~0.05 ms for Pr^{3+} ions), rendering Tb^{3+} ions suitable for energy storage [3,17,18].

To date, continuous-wave (CW) operation of Tb visible lasers has already been investigated in many materials (such as $LiYF_4$, $LiLuF_4$, $LiTbF_4$, and YAG) [14,18–20]. In the green spectral region, a maximum CW output power of ~1.1 W and a slope efficiency of 63% have been reported using a 15% $Tb:LiYF_4$ crystal [21]. Furthermore, a passively Q-switched operation of a Tb^{3+} laser has been realized to obtain high-peak-power laser pulses, which produced a pulse energy of 19.2 μJ and a peak power of 6.6 W at 38.7 kHz [22]. A compact deep ultraviolet frequency-doubled $Tb:LiYF_4$ laser at 272 nm has also been reported, which produced a pulse energy and peak power of 100 μJ and 320 W, respectively [23].

#434010 https://doi.org/10.1364/OE.434010
Journal © 2021 Received 17 Jun 2021; revised 25 Aug 2021; accepted 26 Aug 2021; published 20 Sep 2021

Optics EXPRESS

Compared with those of passive Q-switching schemes, the advantages of active Q-switching include a shorter pulse width, higher peak power, and an easily controllable pulse repetition rate of the generated laser pulses. The most commonly used active Q-switching techniques are acousto-optic (AO) Q-switching and electro-optic (EO) Q-switching. Recently, an AO Q-switched Tb:$LiYF_4$ laser was reported, which produced a pulse energy of 148 μJ and a peak power of 580 W at a repetition rate of 3 kHz [24]. An electro-optically Q-switched laser, based on a rare earth Pr^{3+} ion-doped material, was also reported, which produced a pulse width of 120 ns and a pulse energy of 1.6 mJ [25]. Theoretically, EO Q-switching has a faster switching speed and can achieve a lower repetition rate, and to obtain a higher peak power, we used EO Q-switching in out study. In addition, the Tb:$LiYF_4$ crystal has a tetragonal structure. Therefore, it can generate linearly polarized light directly. We employed EO Q-switching due to the combination of advantages a simple cavity structure that provides a larger modulation depth.

In this study, we successfully demonstrated that the electro-optically Q-switched Tb:$LiYF_4$ laser directly generates pulsed laser radiation at 544 nm. Using an optically pumped semiconductor laser at 488 nm, the output laser properties at repetition rates in the range from 200 Hz to 50 kHz were investigated in detail. A peak power of approximately 800 W was generated with a pulse width of 248 ns at an absorbed pump power of 1.6 W and a repetition rate of 200 Hz. To the best of our knowledge, the demonstrated electro-optically Q-switched Tb^{3+} laser, among all the Tb^{3+} lasers, has produced the highest peak power to date.

2. Experimental results and discussion

2.1. Experimental setup

Figure 1 shows the experimental setup of the electro-optically Q-switched Tb:$LiYF_4$ laser. A frequency-doubled optically pumped semiconductor laser (2ω-OPSL, Coherent Genesis CX-STM), which can provide a high-quality laser beam with M^2 ~1.05 and a maximum output power of 3 W at 488 nm wavelength, was employed as the pump source. To match the largest absorption cross section and subsequently ensure a high absorption efficiency, a λ/2 waveplate was placed between the pump source and the focusing lens. We measured the absorption efficiency of the crystal to be ~52%.

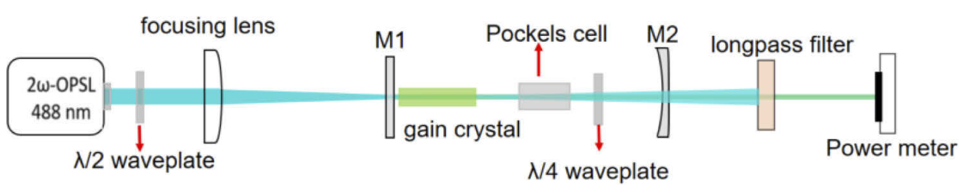

Fig. 1. Optical setup of the EO Q-switched Tb:$LiYF_4$ laser.

The pump beam was focused into the Tb:$LiYF_4$ crystal with a lens of f=500 mm through the plane input coupling mirror (M1, coated with HR at lasing wavelength and HT at pump wavelength). A concave mirror (M2, PR coated at lasing wavelength (T_{oc}~5%)) with a radius curvature of 100 mm was employed as the output coupler. An a-cut 10% Tb:$LiYF_4$ crystal was used as the gain medium (30 mm length, visible-AR coated on both surfaces, commercially ordered from EKSMA Optics). The crystal was placed as close as possible to M1 and installed in a copper heat sink, cooled to 15 °C. For the Q-switched operation, a KD_2PO_4 Pockels cell (PC12SR-515/532, commercially ordered from EKSMA Optics) with dimensions of ϕ 5 mm × 30 mm was placed behind the Tb:$LiYF_4$ crystal. The Pockels cell exhibited single-pass optical transmission > 96% at 544 nm. To reverse the population storage and release time, a λ/4 waveplate was inserted between the Pockels cell and the output coupler. The waveplate blocked the laser oscillation in the case of non-voltage on the Pockels cell, thus preventing the Pockels cell from receiving high voltage for a long period of time. The physical length of the resonator was approximately 100 mm, and the length of cavity was adjusted to be as short as possible. The diameter of the pump spot on the crystal was about 80 μm. For our resonator, the calculated Gaussian mode diameter on the gain medium was about 148 μm, based on an ABCD matrix. No additional optical components, such as a polarizer, were inserted into the cavity to minimize the intracavity losses. However, we inserted a long-pass filter (FEL0500, Thorlabs) in front of the power meter to block any unabsorbed pump light.

2.2. Green laser operation of Tb:LiYF$_4$

First, we provide the investigation results of the average output power in the CW and Q-switched operations in Fig. 2(a). The laser emission was pi-polarized. A maximum CW output power of 178 mW was obtained at an absorbed pump power of 1.6 W. The corresponding absorbed threshold power and slope efficiency were 765 mW and 20%, respectively. Further, the average output powers under different repetition rates in the Q-switched operation were recorded. The maximum average output power of 40 mW was generated at a repetition rate of 200 Hz. The threshold and corresponding slope efficiency were 1.4 W and 17%, respectively. In the experiment, the laser spots observed by the naked eye were almost circular and showing typical TEM$_{00}$ mode at all power levels.

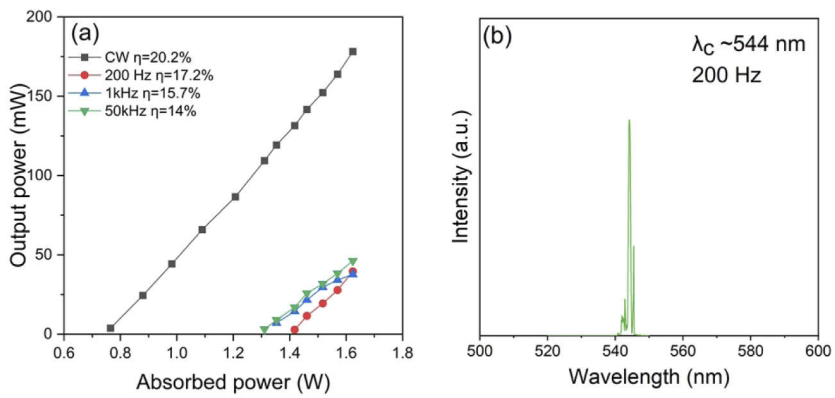

Fig. 2. (a) Average output power of the CW and EO Q-switched Tb:LiYF$_4$ laser and (b) output spectrum.

The output laser spectra of the CW and EO Q-switched Tb:LiYF$_4$ lasers were measured using an optical spectrum analyzer (Q8381A, Advantest). In our experiments, the measured spectra were almost identical for the CW and Q-switched operation. A typical output spectrum of the Q-switched Tb:LiYF$_4$ laser is shown in Fig. 2(b). The center wavelength is located at 544 nm with a spectral line width of ~0.8 nm. In addition, to determine whether changes in the repetition rate would affect the spectrum, we measured the spectra of 200 Hz and 1 kHz respectively, and we found that the results were almost unchanged.

The temporal characteristics of the EO Q-switched Tb:LiYF$_4$ laser were recorded using a 3 GHz bandwidth oscilloscope (MDO4024C, Tektronix) with a silicon-based detector (Thorlabs DET10A/M, rise time ~1 ns). Typical pulse trains at 50 kHz, 1 kHz, and 200 Hz are shown in Figs. 3(a–c). The EO Q-switched laser worked stably at each repetition rate at the maximum absorbed pump power of 1.6 W. To better describe the stability of the laser pulses, we have quantified the pulse fluctuation. According to the calculations, the RMS pulse-to-pulse amplitude fluctuations at the rates of 200 Hz, 1 kHz, and 50 kHz were 7%, 8%, and 8%, respectively. Owing

Optics EXPRESS

to the limitations of the EO driver, the waveform becomes unstable when the repetition frequency is higher than 50 kHz. Figure 3(d) shows a typical single-pulse waveform at a repetition rate of 200 Hz. The shortest pulse width was measured to be approximately 248 ns.

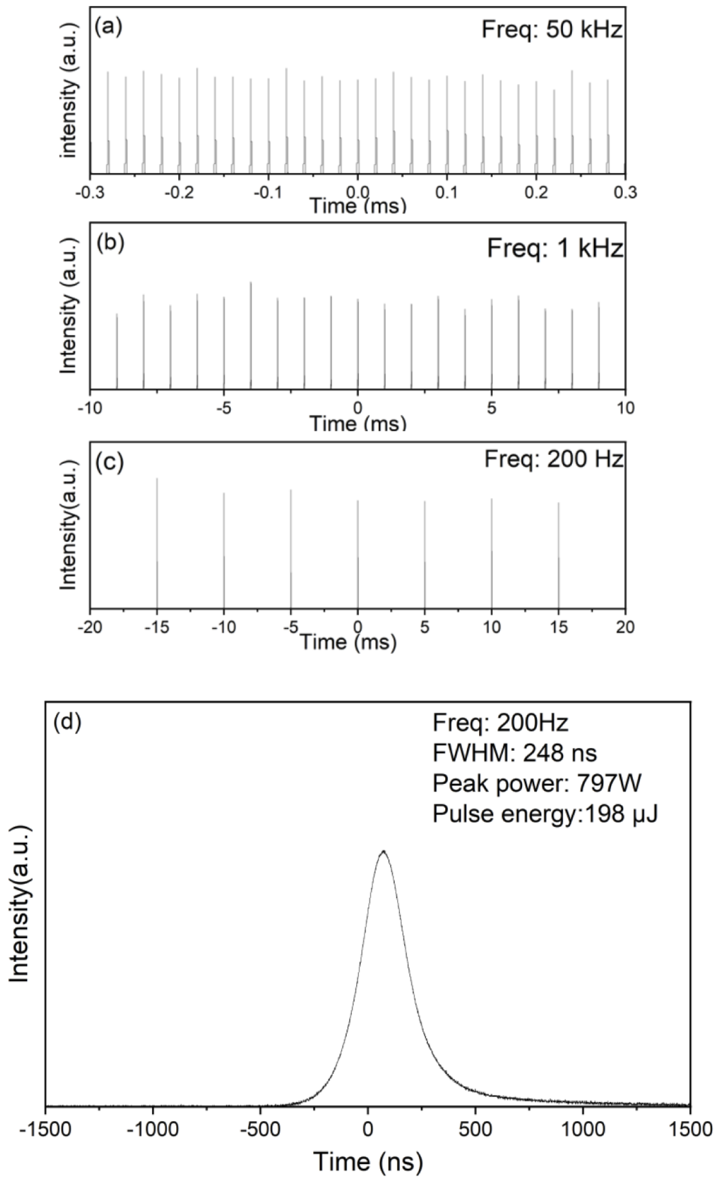

Fig. 3. (a-c) Variation of the typical pulse train with different frequencies at the absorbed pump power of 1.6 W. (d) Pulse waveform at the 200 Hz repetition rate.

Figure 4(a) shows the dependence of the pulse energy on the absorbed pump power. For both repetition frequencies, the pulse energy increases almost linearly with an increase in the absorbed pump power in a range from 1.3 W to 1.6 W. At a repetition rate of 200 Hz, a maximum pulse energy of 198 μJ was obtained. Figure 4(b) displays the measured pulse width and the calculated peak power as functions of the absorbed power. At each repetition rate, the peak power increased almost linearly with an increase in the absorbed pump power, while the pulse width gradually decreased. The shortest pulse width was 248 ns corresponding to a peak power of 797 W.

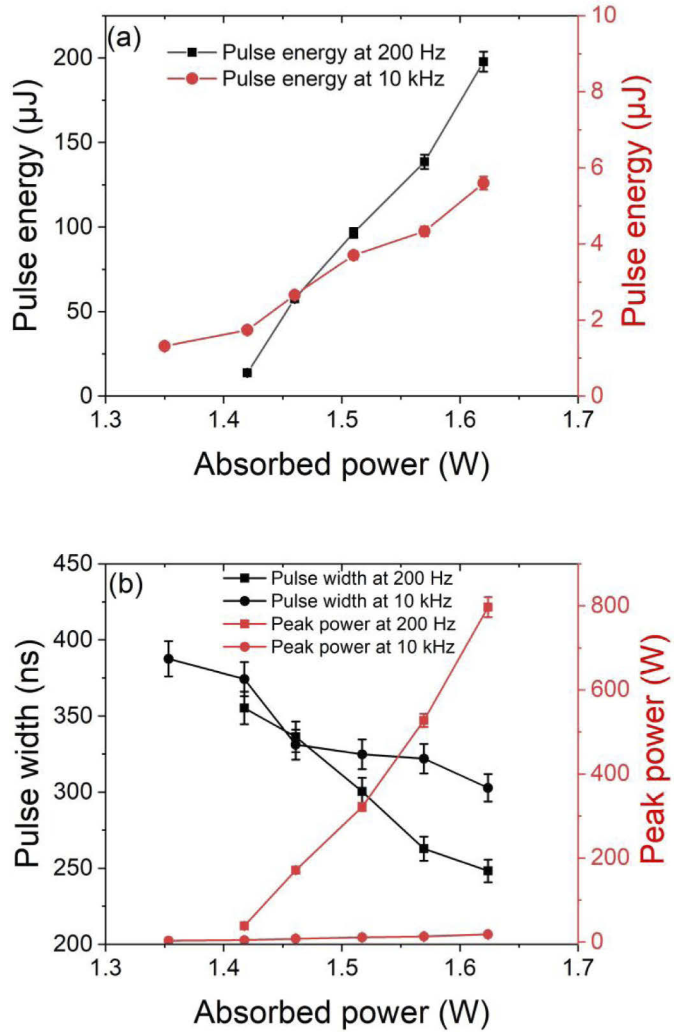

Fig. 4. (a) Pulse energy. (b) Peak power and pulse width plotted with the absorbed pump power under different repetition rates.

Figure 5 illustrates the pulse width and peak power achieved in the Q-switched Tb:LiYF$_4$ laser, operated at several repetition rates at the maximum absorbed power of 1.6 W. As the repetition frequency decreased in a range from 50 kHz to 200 Hz, the pulse width decreased in a range from 388 ns to 248 ns, while the peak power steadily increased in a range from 2.4 W to 797 W. The maximum peak power of 797 W was higher than that of the AO Q-switched Tb:LiYF$_4$ laser.

2.3. Discussion

In our experiment, the shortest pulse widths remained almost unchanged when the pulse repetition frequency was decreased from 800 Hz to below 200 Hz. We attribute this to the small energy storage difference for repetition rates below 800 Hz at the currently available pump power level.

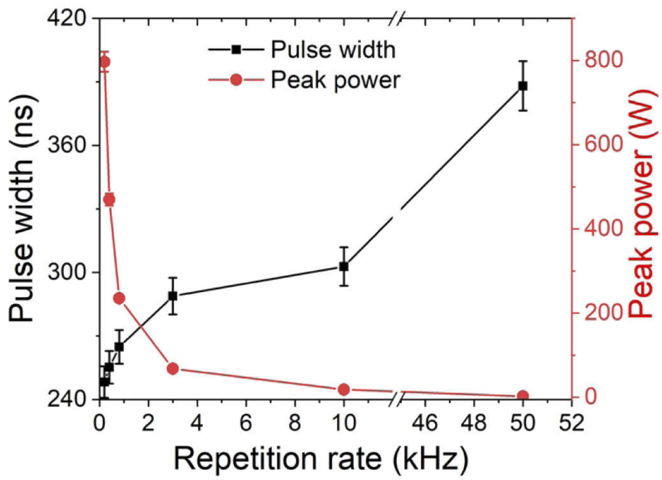

Fig. 5. Pulse width and peak power plotted with a repetition rate at the absorbed pump power of 1.6 W.

The storage efficiency of the Q-switched laser can be expressed as [26,27]:

$$\eta_s = t_s/t_m[1 - \exp(-t_m/t_s)], \tag{1}$$

where t_s is the upper-level lifetime and t_m is the pulse period. Using Eq. (1), when the repetition rate is 50 kHz, η_s is approximately 99.8%. Further, when the repetition rate decreased from 800 Hz to 200 Hz, the storage efficiency decreased from 67.2% to 63.2%. Here, the upper-level lifetime of the Tb:$LiYF_4$ crystal is considered to be approximately 5 ms. When the pulsing interval is larger than 5 ms, the spontaneous emission and non-radiative relaxation processes consume the stored energy and then degrade the pulse energy. In other words, the stored energy tends to saturate for repetition rates lower than 200 Hz.

Theoretically, the shortest pulse width (t_p) achieved from a Q-switched laser can be calculated according to the following equation [28]:

$$t_p = \frac{t_r}{\delta}[\frac{\ln z}{z(1 - a\ln a)}], \tag{2}$$

where t_r and δ are the round-trip time and round-trip loss, respectively, and z represents a dimensionless value that is calculated by z=$2g_0l$, where g_0 and l are the small signal gain coefficient and crystal length, respectively. Similarly, a is another dimensionless value calculated by a=$(z$-$1)/zlnz$. The small signal gain (g_0) can be expressed as formula (3):

$$g_0 = \sigma_e\tau_f\eta_Q\eta_S\eta_B P_{abs}/h\nu_L V, \tag{3}$$

where σ is the emission cross section of Tb:$LiYF_4$, τ_f is the life time of Tb:$LiYF_4$, η_Q is the quantum efficiency [29], and η_S and η_B are the Stokes factor and overlap efficiency, respectively. Further, P_{ab} and $h\nu_L$ are the absorbed pump power and photon energy emitted at the laser transition, respectively, and V is the volume of the pump beam in the crystal. Using these parameters, the value of the small signal gain g_0 is not difficult to calculate, and we obtained it to be about 0.14 cm^{-1}. The parameters used for the calculation are summarized in Table 1. Based on these parameters, the theoretical value of the shortest pulse width was calculated to be approximately 130 ns [29], which is shorter than our experimental value of 248 ns. This difference from the theoretical value is possibly due to several factors, such as ignored large internal losses introduced by the scattering centers of the crystal, imperfect coating, mode matching, and possible alignment deviation. Moreover, it should be noted that, because of the ESA and ETU effects in Tb: $LiYF_4$[14,30,31], the inversion value is degraded. Thus, the actual gain value cannot attain the ideal value.

Table 1. Parameters required to calculate pulse width

Parameters	Value
Round trip time (t_r)	0.84 [ns]
Round trip loss (δ)	0.2
Small signal gain (g_0)	0.14 [cm^{-1}]
Crystal length (l)	3 [cm]
Emission cross section (σ)	0.8×10^{-21} [cm^2] [20]
Life time (τ_f)	4.9 [ms]
Quantum efficiency (η_Q)	0.65 [29]
Stokes factor (η_S)	0.89
Overlap efficiency (η_B)	1
Absorbed pump power (P_{ab})	1.6 [W]
Photon energy emitted at the laser transition ($h\nu_L$)	3.7×10^{-19} [J]
Volume of the pump beam in the crystal (V)	7.85×10^{-4} [cm^3]

Figure 3(b) indicates that the peak power can be further increased with an increase in the absorbed pump power. In our experiment, the maximum absorbed pump power was limited to only 1.6 W. Therefore, we believe that, by using a pump source with a higher output power and optimizing the mode matching, as well as precisely adjusting the output transmittance, the pulse width can be further decreased, thereby increasing the peak power to beyond several kW.

3. Conclusion

To the best of our knowledge, we have demonstrated, for the first time, the electro-optically Q-switched operation of a Tb:$LiYF_4$ green laser in this paper. A stable Q-switched operation was realized under a wide range of repetition rates from 200 Hz to 50 kHz. The highest peak power of 797 W was achieved at an absorbed power of 1.6 W and a 200 Hz repetition rate. The corresponding pulse width and pulse energy were 248 ns and 198 µJ, respectively. Further enhancement of the peak power can be realized by increasing the pump power and reducing the intracavity loss.

Funding. Japan Society for the Promotion of Science (18H01204).

Disclosures. The authors declare no conflicts of interest.

Data availability. Data underlying the results presented in this paper are not publicly available at this time but may be obtained from the authors upon reasonable request.

References

1. V. Bhatia, S. J. Gregorski, D. Pikula, S. C. Chaparala, D. A. S. Loeber, J. Gollier, J. D. Gregorski, M. Hempstead, Y. Ozeki, Y. Hata, K. Shibatani, F. Nagai, N. Mori, Y. Nakabayashi, N. Mitsugi, and S. Nakano, "Efficient and compact green laser for micro-projector applications," J. Soc. Inf. Disp. **17**(3), 271–277 (2009).
2. T. Hager, U. Strauß, and C. Eichler, "Power blue and green laser diodes and their applications," Proc. SPIE **8640**, 86400G–86401 (2013).
3. C. Kränkel, "Out of the blue: Semiconductor laser pumped visible rare-earth doped lasers," Laser Photonics Rev. **10**(4), 548–568 (2016).
4. L. J. Walsh, "The current status of laser applications in dentistry," Aust. Dent. J. **48**(3), 146 (2003).
5. B. Azadgoli and R. Y. Baker, "Laser applications in surgery," Ann. Transl. Med. **4**(23), 452 (2016).

Optics EXPRESS

6. S. Engler, R. Ramsayer, and R. Poprawe, "Process studies on laser welding of copper with brilliant green and infrared lasers," Phys. Procedia **12**(B), 339–346 (2011).
7. J. Han, T. Luo, L. Sun, C. Ding, M. Xia, and K. Yang, "Research of application of high-repetition-rate green laser in underwater imaging system," Proc. SPIE **8905**, 89051Y–89051 (2013).
8. S. Pandya, J. Yu, and D. Parker, "Engineering emissive europium and terbium complexes for molecular imaging and sensing," Dalton Trans. **23**(23), 2757–2766 (2006).
9. S. Masui, T. Miyoshi, T. Yanamoto, and S. Nagahama, "Blue and green laser diodes for large laser display," *CLEO Pac. Rim* SA 1–3 (2013).
10. J. Bovatsek, A. Tamhankar, R. S. Patel, N. M. Bulgakova, and J. Bonse, "Thin film removal mechanisms in ns-laser processing of photovoltaic materials," Thin Solid Films **518**(10), 2897–2904 (2010).
11. S. Konno, T. Kojima, S. Fujikawa, and K. Yasui, "High-brightness 138-W green laser based on an intracavity-frequency-doubled diode-side-pumped Q-switched Nd:YAG laser," Opt. Lett. **25**(2), 105–107 (2000).
12. C. Czeranowsky, E. Heumann, and G. Huber, "All-solid-state continuous-wave frequency-doubled Nd:YAG–BiBO laser with 2.8-W output power at 473 nm," Opt. Lett. **28**(6), 432–434 (2003).
13. U. Osterberg and W. Margulis, "Dye laser pumped by Nd:YAG laser pulses frequency doubled in a glass optical fiber," Opt. Lett. **11**(8), 516–518 (1986).
14. P. W. Metz, D.-T. Marzahl, A. Majid, C. Kränkel, and G. Huber, "Efficient continuous wave laser operation of Tb^{3+}-doped fluoride crystals in the green and yellow spectral regions," Laser Photonics Rev. **10**(2), 335–344 (2016).
15. T. Lu, J. Ma, M. Huang, Q. Yang, X. Zhu, and W. Chen, "High-Efficient Nd:YLF Q-Switched Laser Operating at 523.5 nm," Chinese Phys. Lett. **31**(7), 074208 (2014).
16. Z. Heng-Li, L. Xiao-Meng, L. Dai-Jun, S. Peng, A. Schell, C. R. Haas, and D. Ke-Ming, "A Compact 532-nm Source by Frequency Doubling of a Diode Stack End-Pumped Nd:YAG Slab Laser," Chinese Phys. Lett. **24**(10), 2846–2848 (2007).
17. J. J. Degnan, "Theory of the optimally coupled Q-switched laser," IEEE J. Quantum Electron. **25**(2), 214–220 (1989).
18. H. Jenssen, D. Castleberry, D. Gabbe, and A. Linz, "Stimulated emission at 5445 Å in Tb3+: YLF," IEEE J. Quantum Electron. **9**(6), 665 (1973).
19. J. Liu, Q. Song, D. Li, Y. Ding, X. Xu, and J. Xu, "Spectroscopic properties of Tb:$Y_3Al_5O_{12}$ crystal for visible laser application," Opt. Mater. **106**, 110001 (2020).
20. E. Castellano-Hernández, S. Kalusniak, P. W. Metz, and C. Kränkel, "Diode-pumped laser operation of Tb3+:LiLuF4 in the green and yellow spectral rang," Laser Photonics Rev. **14**(2), 1900229 (2020).
21. H. Chen, H. Uehara, H. Kawase, and R. Yasuhara, "Efficient visible laser operation of Tb:$LiYF_4$ and LiTb:YF_4," Opt. Express **28**(8), 10951–10959 (2020).
22. H. Chen, W. Yao, H. Uehara, and R. Yasuhara, "Graphene Q-switched Tb:$LiYF_4$ green laser," Opt. Lett. **45**(9), 2596–2599 (2020).
23. H. Chen, H. Uehara, and R. Yasuhara, "Compact deep ultraviolet frequency-doubled Tb:$LiYF_4$ lasers at 272 nm," Opt. Lett. **45**(19), 5558–5561 (2020).
24. H. Chen, W. Yao, H. Uehara, and R. Yasuhara, "Actively Q-switched Tb:LiYF4 green lasers," Appl. Phys. Express **14**(6), 062002 (2021).
25. H. Jeĺınkova, M. Fibrich, M. Čech, P. Hiršl, K. Nejezchleb, and V. Škoda, "Electro-optically Q-switched Pr:YAP laser generating at 747 nm," Laser Phys. Lett. **6**(7), 517–520 (2009).
26. Y. Wang, T. Zhao, D. Shen, H. Zhu, J. Zhang, and D. Tang, "Resonantly pumped Q-switched Er:YAG ceramic laser at 1645 nm," Opt. Express **22**(20), 24004–24009 (2014).
27. N. P. Barnes, "Solid-state lasers from an efficiency perspective," IEEE J. Sel. Top. Quantum Electron. **13**(3), 435–447 (2007).
28. W. Koechner, *Solid-State Laser Engineering*, (VI, ed. (Springer, 2006).
29. V. Vasyliev, E. G. Víllora, Y. Sugahara, and K. Shimamura, "Judd-Ofelt analysis and emission quantum efficiency of Tb-fluoride single crystals: $LiTbF_4$ and $Tb_{0.81}Ca_{0.19}F_{2.81}$," J. Appl. Phys. **113**(20), 203508 (2013).
30. T. Yamashita and Y. Ohishi, "Amplification and lasing characteristics of Tb^{3+}—Doped fluoride fiber in the 0.54-µm band," Jpn. J. Appl. Phys. **46**(41), L991–L993 (2007).
31. T. Yamashita, G. Qin, T. Suzuki, and Y. Ohishi, "A new green fiber laser using Terbium-doped fluoride fiber," *OFC Conference JWA18*, 2008.